Macromolecules

pubs.acs.org/Macromolecules Article

Cyclic Poly(Thioester Amide)s via Ring-Opening Copolymerization of Aziridines and Phthalic Thioanhydride: Mechanistic Insights and Enhanced Properties for Sustainable Materials

Jiaojiao Qin, Zhun Xu, Huan Wang, and Xiaoyan Tang*

Cite This: Macromolecules 2025, 58, 7686−7696 Read Online

ACCESS | Metrics & More | Article Recommendations | Supporting Information

ABSTRACT: Ring-opening copolymerization renders aziridines promising candidates for constructing *N*-containing polymers; however, producing polymers with predicted molar masses and defined sequence structures remains challenging. Here, we present a strategy for synthesizing poly(thioester amide)s (PTEAs) via ROCOP of *N*-alkyl aziridines and phthalic thioanhydride. Remarkably, perfectly alternating copolymerization was achieved by the synergistic catalysis of a phosphazene base and a protic initiator, delivering cyclic PTEAs with a molar mass of up to 188.4 kDa. Model reaction and chain extension experiments supported the rapid *S*-to-*N* acyl shift after aziridine ring-opening and spontaneous ring-closure upon applying an external stimulus. Notably, liquid-phase transmission electron microscopy confirmed the linear or cyclic topology before or after the postprocessing by spatially resolving the morphology of transient conformations. The in-chain thioester bonds endow polymers with enhanced thermal and optical properties compared to their poly(ester amide) counterparts, along with desirable degradability and biocompatibility, establishing a robust foundation for developing PTEAs as sustainable and functional biomedical materials.

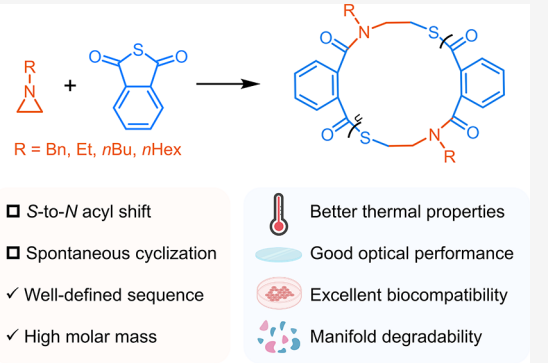

INTRODUCTION

Aziridines have ignited considerable interest over the past decade due to their remarkable potential as important intermediates in organic synthesis and bioactive compounds in pharmacology.[1,2] The strain stemming from the three-membered ring endows aziridines with heightened reactivity compared with other saturated nitrogen heterocycles, rendering them valuable building blocks for constructing nitrogen-containing molecules. Albeit bearing similar structures and comparable ring strain, aziridines and epoxides exhibit disparate chemical properties owing to the reduced electronegativity of nitrogen and the increased nucleophilicity of nitrogen's lone pair of electrons, particularly evident in polymer chemistry.[3,4] Generally, the polymerization of aziridines relies less on the use of Lewis acids than that of epoxides and is strongly affected by the substituents on nitrogen. Based on previous reports on the ring-opening polymerization (ROP) of aziridines, it can be concluded that aziridines with hydrogen or electron-donating substituents tend to homopolymerize via a cationic mechanism, accompanied by poor control over molar mass and structural regularity.[5,6] In contrast, aziridines with electron-withdrawing substituents, especially sulfonyl groups, are regarded as activated monomers with an augmentation of the electrophilicity of carbon atoms on the ring, making them prone to homopolymerize in an anionic mechanism along with a living polymerization characteristic.[7] Nevertheless, advancements in the polymerization method, molar mass control, and structural regularity for aziridines have lagged far behind those for epoxides, despite the potential structural diversity and attractive applications of the resulting polymers.

Ring-opening copolymerization (ROCOP) of heterocycles and heteroallenes has emerged as a powerful method for preparing degradable polymers, enabling the introduction of various degradable moieties into polymer main chains through different combinations of simple monomers compared to ROP of cyclic monomers.[8−10] This approach features a high atom economy and controlled polymerization process performed under mild conditions, in contrast with step-growth polymerization. ROCOP of aziridines with CO,[11] CO_2,[12] or cyclic anhydrides[13−19] provides a facile route to acquire *N*-containing polymers with diverse functionalities, such as poly-*β*-peptoids, polyurethanes, and poly(ester amide)s (PEAs), respectively. Among them, cyclic anhydrides are enticing comonomers due to their nontoxic nature, ease of handling, and economic

Received: February 24, 2025
Revised: April 24, 2025
Accepted: April 25, 2025
Published: May 7, 2025

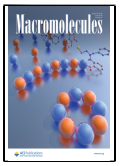

https://doi.org/10.1021/acs.macromol.5c00511
Macromolecules 2025, 58, 7686−7696

Scheme 1. Copolymerization of Aziridines and Phthalic Thioanhydride to Produce Cyclic Poly(Thioester Amide)s with Improved Properties

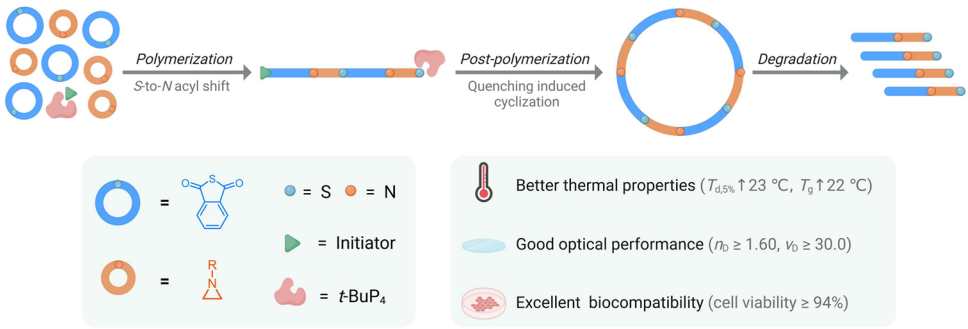

Table 1. Results of Copolymerization between Az^{Bn} and PTA[a]

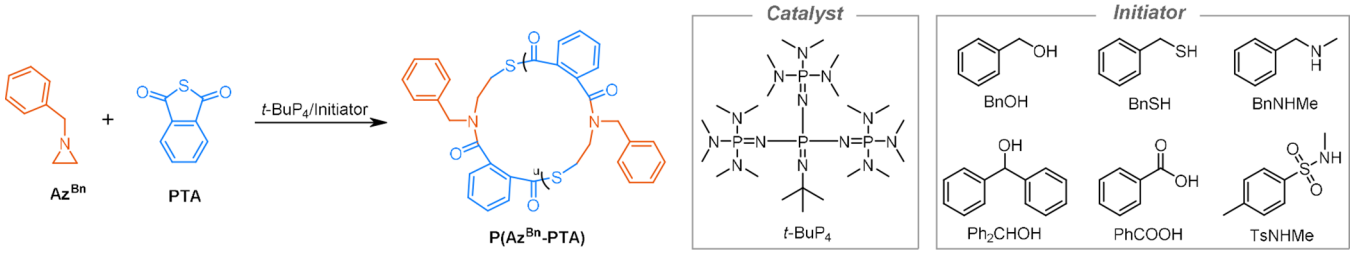

entry	catalyst/initiator	$[Az^{Bn}]_0/[PTA]_0/[t\text{-}BuP_4]_0/[I]_0$	temp. (°C)	$[Az^{Bn}]_0$ (mol L^{-1})	time (h)	conv. of Az^{Bn}[b] (%)	selectivity[b] (%)
1		1/1/0/0	90	2	136	98	59
2	BnOH	100/100/0/1	90	2	24	90	48
3	$t\text{-}BuP_4$	200/200/1/0	90	1	8	94	84
4	$t\text{-}BuP_4$/BnOH	100/100/1/1	90	1	12	99	63
5	$t\text{-}BuP_4$/BnOH	100/100/1/1	RT	1	18	87	99
6	$t\text{-}BuP_4$/BnSH	100/100/1/1	RT	1	18	85	99
7	$t\text{-}BuP_4$/BnNHMe	100/100/1/1	RT	1	18	91	99
8	$t\text{-}BuP_4$/Ph_2CHOH	100/100/1/1	RT	1	18	97	99
9	$t\text{-}BuP_4$/PhCOOH	100/100/1/1	RT	1	24	33	99
10	$t\text{-}BuP_4$/TsNHMe	100/100/1/1	RT	1	24	0	
11	$t\text{-}BuP_4$/BnNHMe	100/0/1/1	RT	2	168	0	
12	$t\text{-}BuP_4$	100/100/1/0	RT	2	48	0	
13	BnNHMe	100/100/0/1	RT	2	192	54	62

[a]All polymerizations conducted in 1,4-dioxane; I, initiator; RT, room temperature. [b]The conversion of Az^{Bn} and alternating selectivity was determined by ^1H NMR in $CDCl_3$ using the integrals of the characteristic signals.

viability. Moreover, the incorporation of degradable ester bonds and the capacity to vary backbone structures via ring-opening of anhydrides make the resulting PEAs promising candidates for applications in degradable commodity packaging and biomedical materials.[20,21]

In this context, we sought new opportunities for integrating aziridines into the construction of polymers with well-defined structures and intriguing properties through ROCOP, given the ready availability and enormous unexploited potential of aziridines. To this end, we chose cyclic thioanhydride, an analogue of cyclic anhydride, as the comonomer based on the following considerations. First, the resultant poly(thioester amide)s (PTEAs) featuring alternately distributed thioester and amide bonds in the polymer main chain represent novel structures that are challenging to achieve by traditional methods, thus fully embodying the advantages of the ROCOP approach. To date, only one study regarded copolymerization of *N*-tosylaziridine and phthalic thioanhydride (PTA), which necessitated 2.5 times equivalent of PTA to aziridine to avoid self-propagation of aziridine due to the similar active species and polymerization conditions required for ROP and ROCOP of activated aziridines, resulting in PTEAs with much lower molar masses than theoretical values.[22] Second, incorporating sulfur atoms is an effective strategy for improving the thermal and mechanical properties,[23−25] as well as the degradability of polymers,[26−29] while imparting novel features such as optical properties,[30−35] dynamic properties,[36] and heavy-metal absorption.[37−39] However, the specific impact of thioester in collaboration with amide bonds on the thermomechanical performance and particularly the degradability of polymers is unknown, let alone the other appealing properties that remain to be explored. Third, both the sequence structure and molar mass are pivotal to material performance, including crystallinity, degradability, Abbe number, etc.[23,32,40] Achieving defined sequence and topology of polymers is mandatory for ensuring stable material performance and facilitating their applicability in high-end fields but is plagued by the irritating *O*/*S* scrambling in ROCOP.[41−45]

https://doi.org/10.1021/acs.macromol.5c00511
Macromolecules 2025, 58, 7686−7696

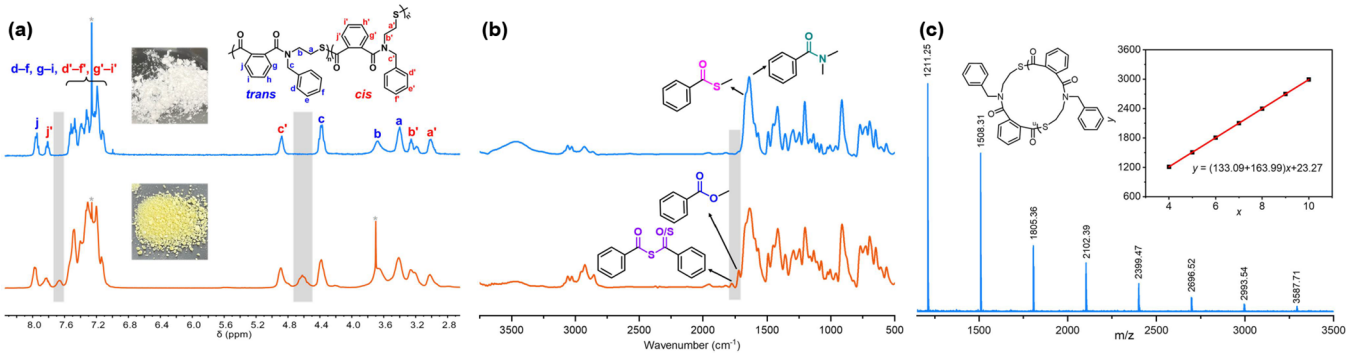

Figure 1. Comparison between catalyst-mediated and spontaneous copolymerization. (a) Overlay of ^{1}H NMR spectra in $CDCl_3$ alongside photographs of the corresponding polymers, with solvent peaks denoted by asterisks, and (b) overlay of FTIR spectra of polymers obtained at 90 °C without catalyst (orange; entry 1, Table 1) and at RT catalyzed by 0.25 mol % *t*-BuP_4/BnNHMe (blue; entry 7, Table 1). (c) MALDI-TOF MS spectrum of the polymer obtained at RT catalyzed by 0.25 mol % *t*-BuP_4/BnNHMe (entry 7, Table 1).

Considering the dilemma encountered in ROCOP of *N*-tosylaziridine and PTA, and motivated by our previous work on the spontaneous copolymerization of *N*-alkyl aziridines and phthalic anhydride (PA),[19] we commence with the copolymerization between the less active *N*-alkyl aziridines and PTA in an anionic fashion to suppress the successive insertion of aziridines during the ROCOP process, as *N*-alkyl aziridines prefer to homopolymerize through a cationic mechanism in the presence of a strong Lewis acid catalyst.[6] In this work, we achieved perfectly alternating copolymerization of *N*-alkyl aziridines and PTA, delivering PTEAs with complete cyclic topology and without erroneous linkages (Scheme 1). The number-average molar mass (M_n) of the resultant PTEAs reached up to 188.4 kDa, the highest value observed among ROCOP toward thioesters,[28] making it possible to "see" the individual cyclic macromolecule via liquid-phase transmission electron microscopy (LP-TEM). We thoroughly investigated the influence of the temperature, catalyst, and initiator on polymer composition and topology. Moreover, we implemented exhaustive kinetic and mechanism studies to elaborate on the polymerization and cyclization processes. Significant improvements in thermal and optical properties were observed when comparing the resulting PTEAs with their PEA analogs. At last, we revealed the degradability and biocompatibility of PTEAs for the first time, paving the way for their potential application in the biomedical field.

RESULTS AND DISCUSSION

Spontaneous ROCOP of *N*-Benzylaziridine (Az^{Bn}) and PTA. At the outset, we performed the copolymerization of Az^{Bn} and PTA in 1,4-dioxane at 90 °C (entry 1, Table 1), following a similar approach to our previous work on the copolymerization of Az^{Bn} and PA, which yielded cyclic PEAs with high molar mass and alternating selectivity via a catalyst-free strategy.[19] Our attempts revealed that the ROCOP of Az^{Bn} and PTA did occur without a catalyst due to the tendency of nucleophilic Az^{Bn} and electrophilic PTA to react with each other. However, there was a notable decrease in the polymerization rate, along with evident side reactions. Specifically, achieving a comparable conversion of Az^{Bn} required 136 h in copolymerization with PTA, whereas it only took 8 h in copolymerization with PA under identical conditions. The distinct reactivity between PTA and PA could be ascribed to the higher intrinsic reactivity of acyl in PA toward nucleophilic attack, owing to the higher electronegativity of oxygen.[46] Additionally, the alternating selectivity observed during the copolymerization process closely approximated the value of the final isolated yellow copolymer (59%, calculated from the ^{1}H nuclear magnetic resonance (NMR) spectrum, with 4.62 ppm representing the erroneous linkages in the bottom spectrum in Figure 1a for instance), but was considerably lower than the value (91%) calculated from the ratio of the final conversion of PTA (89%) to Az^{Bn} (98%). This suggested that more violent and complicated side reactions, besides the consecutive enchainment of Az^{Bn} (the only disturbance in the ROCOP of Az^{Bn} and PA resulting in an alternating selectivity of 92%), occurred throughout this entire copolymerization process.

The poor selectivity results from the abundant thioesters in the main chain, which are more labile than esters because of the weaker resonance between the sulfur atom and carbonyl group, making them susceptible to attacks by strong nucleophiles.[47] Consequently, polymers with low molar masses, high dispersity, and complex structures are often obtained when polymerizing sulfur-containing monomers due to deleterious side reactions, as exemplified by transthioesterification and backbiting side reactions in ROP of thioesters[48,49] and O/S scrambling in ROCOP of epoxides with cyclic thioanhydrides,[50−52] carbonyl sulfide,[53] or carbon disulfide.[54]

To investigate potential side reactions in this case, the copolymer was extensively characterized using ^{13}C NMR (Figure S6), Fourier transform infrared (FTIR; Figure 1b) spectroscopy, and matrix-assisted laser desorption ionization time-of-flight mass spectroscopy (MALDI-TOF MS; Figure S25). Generally, these analyses revealed the presence of C=S, C(=O)−O, and C(=O)−S−C(=O/S) groups and the absence of long polyamine linkage resulting from the consecutive Az^{Bn} enchainment. For detailed information on side reactions occurring during the spontaneous ROCOP between Az^{Bn} and PTA, refer to Figures 1, S6, and S25, along with Scheme S1 in the Supporting Information.

ROCOP of Az^{Bn} and PTA with Organic Bases. Drawing from the strategy applied in ROCOP of Az^{Bn} or *N*-tosylaziridine with PA,[14,19] BnOH and/or organic superbase 1-*tert*-butyl-4,4,4-tris(dimethylamino)-2,2-bis[tris(dimethylamino)phosphoranylid-enamino]-2λ^5,4λ^5-catenadi(phosphazene) (*t*-BuP_4) were employed to accelerate the polymerization and/or increase the alternating selectivity, respectively. As anticipated, the addition of 1 mol % BnOH relative to monomers considerably shortened the reaction time

https://doi.org/10.1021/acs.macromol.5c00511
Macromolecules 2025, 58, 7686−7696

Table 2. Results of Copolymerization between Az^R and PTA[a]

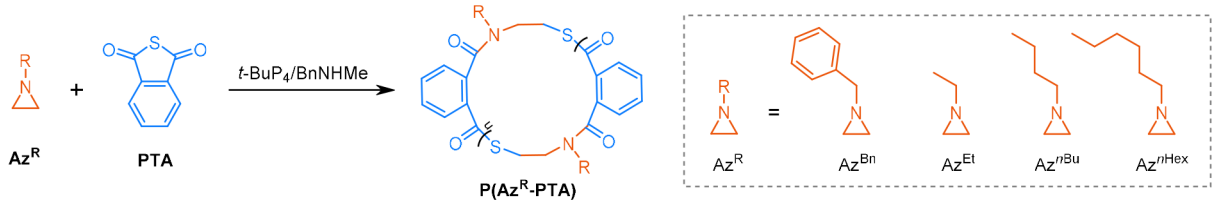

entry	Az^R	$[Az^R]_0/[PTA]_0/[t\text{-}BuP_4]_0/[BnNHMe]_0$	$[Az^R]_0$ (mol L^{-1})	time (h)	conv.[b] (%)	selectivity[b] (%)	$M_{n,theory}$[c] (kDa)	M_n[d] (kDa)	$Đ$[d] (M_w/M_n)
1	Az^{Bn}	25/25/1/1	1	7	95	99	7.4	11.1	1.20
2	Az^{Bn}	50/50/1/1	2	6	99	99	14.9	18.9	1.35
3	Az^{Bn}	100/100/1/1	2	12	99	99	29.7	33.9	1.37
4	Az^{Bn}	200/200/1/1	2	12	91	99	54.1	56.8	1.33
5	Az^{Bn}	300/300/1/1	2	22	93	99	82.9	84.0	1.44
6	Az^{Bn}	400/400/1/1	2	35	94	99	118.9	107.1	1.34
7	Az^{Bn}	1000/1000/1/1	3	48	95	99	282.2	131.4	1.35
8	Az^{Bn}	2500/2500/1/1	3	95	92	99	683.1	188.4	1.36
9	Az^{Bn}	200/200/1/1.4	2	20	94	99	42.4	39.7	1.39
10	Az^{Bn}	200/200/0.6/1	2	32	96	99	59.4	58.8	1.30
11	Az^{Et}	300/300/1/1	2	10	94	99	66.3	76.7	1.40
12	Az^{nBu}	300/300/1/1	2	9	99	99	78.9	73.7	1.33
13	Az^{nHex}	300/300/1/1	2	6	99	99	87.3	53.4	1.32

[a]All polymerizations conducted in 1,4-dioxane at RT. [b]The conversion of Az^R and alternating selectivity was determined by ^1H NMR in $CDCl_3$ using the integrals of the characteristic signals. [c]Calculated number-average molar mass based on feed ratios and conversions: $M_{n,theory} = ([Az^R]_0/[I]_0) \times$ Conv. of $Az^R \times$ (M.W. of Az^R + M.W. of PTA). [d]Determined by SEC equipped with a 9-angle laser light scattering detector using dimethylformamide (DMF) containing 0.1 mol L^{-1} LiBr as the mobile phase.

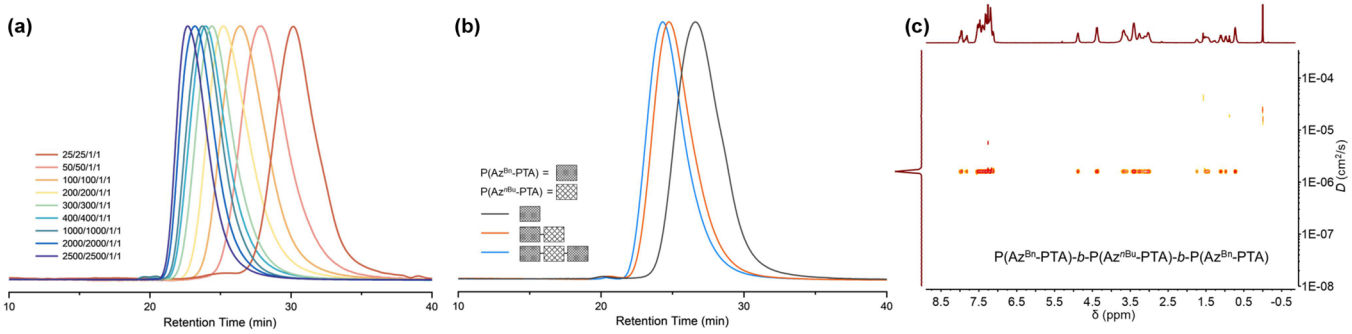

Figure 2. (a) SEC traces of P(Az^{Bn}-PTA) prepared with different $[M]_0/[I]_0$. (b) Evolution of SEC traces of the one-pot, three-step synthesis of block polymers. (c) ^1H DOSY NMR spectrum of the block polymer P(Az^{Bn}-PTA)-*b*-P(Az^{nBu}-PTA)-*b*-P(Az^{Bn}-PTA).

to 24 h to achieve 90% conversion but led to a decreased selectivity of 48% (entry 2, Table 1). Unexpectedly, the polymerization accelerated when adding 0.25 mol % *t*-BuP_4 to an even more dilute polymerization solution, along with a significantly increased selectivity of 84% (entry 3, Table 1), which inferred a strong interaction between PTA and *t*-BuP_4 (Figure S49). Besides, when *t*-BuP_4 and BnOH were used simultaneously, forming a potent catalyst/initiator combination competent in catalyzing the ROP and ROCOP of *N*-sulfonyl aziridines, it resulted in a similar reaction rate as adding *t*-BuP_4 alone and an intermediate selectivity of 63% at 90 °C (entry 4, Table 1).

As is always the case with ROCOP of sulfur-containing monomers, undesirable side reactions can be suppressed by copolymerizing at low temperatures.[40,51,55] To this end, we performed the copolymerization of Az^{Bn} and PTA at room temperature (RT) with a feed ratio of $[Az^{Bn}]_0/[PTA]_0/[t\text{-}BuP_4]_0/[BnOH]_0$ = 100/100/1/1 (entry 5, Table 1). Surprisingly, 87% of Az^{Bn} was converted after 18 h, affording completely alternating P(Az^{Bn}-PTA) in white color, with no erroneous linkage observed in ^1H and ^{13}C NMR spectra (Figures 1a, S3, and S4). As expected, there were two sets of peaks arising from the *cis*−*trans* isomerization of tertiary amides in the main chain, with a *trans*/*cis* ratio of approximately 2/1, which can be assigned by referring to the ^1H−^{13}C HSQC NMR spectrum (Figure S5) and reported PEAs with similar structures.[19,56] In contrast, no reaction occurred between Az^{Bn} and PA at RT with 2 mol % *t*-BuP_4/BnOH under otherwise identical conditions. This reversal of reactivity between PTA and PA in the presence of the catalyst suggests that *t*-BuP_4/BnOH is more conducive to the copolymerization of PTA and Az^{Bn}, which was confirmed by the ^1H NMR titration experiment (Figure S50) and the model reaction (vide infra). Moreover, thiocarboxylate derived from PTA is a more effective nucleophile in facilitating the ring-opening of Az^{Bn} than carboxylate derived from PA, as supported by the faster polymerization rate of PTA than PA when copolymerizing with epoxides.[46]

https://doi.org/10.1021/acs.macromol.5c00511
Macromolecules 2025, 58, 7686−7696

In addition to BnOH, common initiators were screened to test the universality of phosphazene catalysis (entries 5−10, Table 1). The polymerization rate was found to increase in the following order: TsNHMe ≪ PhCOOH ≪ BnSH ≈ BnOH ≈ BnNHMe < Ph_2CHOH under identical conditions, which correlated with the steric hindrance and acidity of initiators and the nucleophilicity of the anions.[57] The less effective TsNHMe and PhCOOH in our system, contrary to their outstanding performance when polymerizing *N*-sulfonyl aziridines, indicated that ring-opening of nonactivated Az^{Bn} was not as facile as proposed in the literature, and carboxylates might not be the key active species functioning in the initiation step.[14,22] To examine our hypothesis, we performed the homopolymerization of Az^{Bn}, and it turned out that the catalyst failed to initiate the self-propagation of Az^{Bn} even after a week under the same conditions as copolymerization (entry 11, Table 1). Strikingly, the MALDI-TOF MS spectrum of P(Az^{Bn}-PTA) revealed the purely cyclic topology without any chain end group in addition to its perfectly alternating sequence (Figure 1c).

The molar masses of polymers allowed for facile tuning by changing the feed ratios of the initiator to the monomer (entries 1−10, Table 2). Size exclusion chromatography (SEC) traces shifted left with decreasing initiator concentrations, with all exhibiting narrow and unimodal distributions (Figures 2a and S21), while completely overlapping SEC traces were observed for P(Az^{Bn}-PTA)s prepared with feed ratios of $[Az^{Bn}]_0/[PTA]_0/[t\text{-}BuP_4]_0/[BnNHMe]_0$ = 200/200/1/1, 200/200/0.6/1, and 200/200/0.4/1, respectively (Figure S22). Moreover, although some deviation from the theoretical molar masses exists for copolymerization with feed ratios lower than 0.1 mol %, the Az^{Bn} conversion could reach 92% with 0.04 mol % *t*-BuP_4/BnNHMe and without sacrificing selectivity (Figure S2), affording copolymers with the highest M_n of 188.4 kDa among thioester-containing polymers via ROCOP (Table S3).[28] Besides, it is noteworthy that the polymerization maintains perfect sequence regularity, regardless of using equivalent or less catalyst relative to the initiator and PTA relative to Az^{Bn} (Figures S27 and S28).

For comparison, we also evaluated the performance of several typical organic bases, including 1,5,7-triazabicyclo[4.4.0]dec-5-ene (TBD), 7-methyl-1,5,7-triazabicyclo[4.4.0]dec-5-ene (MTBD), 1,8-diazabicyclo[5.4.0]undec-7-ene (DBU), 1,3-di-*tert*-butyl-1*H*-imidazol-3-ium-2-ide (*t*-BuNHC), and *t*-BuOK, as well as some nucleophilic initiators effective in copolymerizing cyclic thioanhydrides and episulfides, including bis(triphenylphosphine)iminium chloride (PPNCl), tetraethylammonium chloride (Et_4NCl), and tetrabutylammonium chloride (Bu_4NCl) (Table S1).[58] Overall, the above bases cannot catalyze the polymerization alone, and the activity was significantly lower compared to *t*-BuP_4 when used in conjunction with BnOH. As for the organic ammonium salts, unsatisfactory alternating selectivity (85−87%) was obtained, although a slightly faster reaction was achieved.

Extension to Other *N*-Alkyl Aziridines. Afterward, we applied the optimal polymerization conditions to copolymerize PTA with other *N*-alkyl aziridines [Az^Rs: *N*-ethylaziridine (Az^{Et}), *N*-butylaziridine (Az^{nBu}), and *N*-hexylaziridine (Az^{nHex})] to assess the versatility of this polymerization method and obtain different PTEAs for further exploration of material properties. To our delight, all copolymerizations proceeded smoothly under the catalysis of 0.33 mol % *t*-BuP_4/BnNHMe at RT (entries 11−13, Table 2). The reaction rates surpassed that observed in the copolymerization between Az^{Bn} and PTA, following this order: Az^{Bn} < Az^{Et} < Az^{nBu} < Az^{nHex}. This trend echoed the phenomenon observed in spontaneous copolymerization between Az^R and PA, suggesting the inherently higher reactivity of aziridines with smaller steric hindrance and longer alkyl substituents. The chemical structures and molar masses of the resulting P(Az^R-PTA)s were thoroughly characterized by ^1H NMR, ^{13}C NMR, MALDI-TOF MS, FTIR, and SEC (Figures S7−12, S23, and S29−S32), substantiating well-defined cyclic PTEAs with >99% alternating selectivity and molar masses close to the theoretical values.

Kinetic and Mechanistic Studies. As aforementioned, the presence of phosphazene base and protic initiator resulted in unusual cyclic topology for all four kinds of aziridines, contrary to the linear polymers with initiator as the chain end in previous literature studies.[14,22,59] This raised questions about the roles of the catalyst and initiator and the timing of macrocycle formation. Hence, we designed the following experiments to elucidate how catalysts and initiators function in our system and interfere with the generation of rings. First, taking the copolymerization of Az^{Bn} and PTA as an example, comprehensive kinetic experiments were carried out by systematically varying the concentration of one variable (Az^{Bn}, PTA, *t*-BuP_4, or BnNHMe) while keeping the concentrations of the other three variables constant, in order to determine the reaction order of the variable component. As shown in Figure S33, the polymerization rates accelerated with increasing $[Az^{Bn}]_0$ or $[BnNHMe]_0$ and slowed down with decreasing $[PTA]_0$ or $[t\text{-}BuP_4]_0$. The apparent rate constants (k_{app}) can be determined from the slopes of the linear-fit lines to the semilogarithmic plots of $\ln([M]_0/[M]_t)$ versus time, implying the near first-order kinetics on the concentration of Az^{Bn} and PTA. Subsequently, by plotting ln k_{app} versus the logarithmic value of the initial concentration of variables, the exact reaction orders are determined to be 0.91, 0.77, 0.50, and 1.32 for Az^{Bn}, PTA, *t*-BuP_4, and BnNHMe, respectively, suggesting that the *t*-BuP_4/BnNHMe pair behaves as a discrete catalyst species. In more extreme scenarios, no reaction happened when *t*-BuP_4 was used alone (entry 12, Table 1), suggesting that its non-nucleophilic nature prevents direct initiation of polymerization (Figure S49). Besides, when BnNHMe was used alone, an extremely slow reaction rate and poor selectivity were observed (entry 13, Table 1). This indicates that while it is thermodynamically possible for BnNHMe to attack PTA to induce ring-opening, it is kinetically unfavorable without activation by *t*-BuP_4. Thus, the synergistic effect of the phosphazene base and initiator in polymerization activity and sequence control is underscored.

As for the cyclization mechanism, cyclic polymers were consistently obtained regardless of the reaction conditions, including the solvent (1,4-dioxane, tetrahydrofuran, or toluene), initiator (BnOH, BnSH, BnNHMe, Ph_2CHOH, or PhCOOH, 1 equiv to *t*-BuP_4), and catalyst (*t*-BuP_4, DBU, MTBD, *t*-BuNHC, or *t*-BuOK, 1 equiv. to BnOH; PPNCl, Et_4NCl, or Bu_4NCl) (Table S1). In addition, the influence of the feed order was also taken into account, as different mixing procedures may result in different initiating/propagating pathways.[57] Five mixing procedures were simultaneously implemented and examined by MALDI-TOF MS and NMR methods (Table S2). However, there was no discernible difference between the five mixing procedures regarding cyclic

https://doi.org/10.1021/acs.macromol.5c00511
Macromolecules 2025, 58, 7686−7696

Scheme 2. Proposed Mechanism for ROCOP between Az^R and PTA in the Presence of *t*-BuP_4/BnNHMe

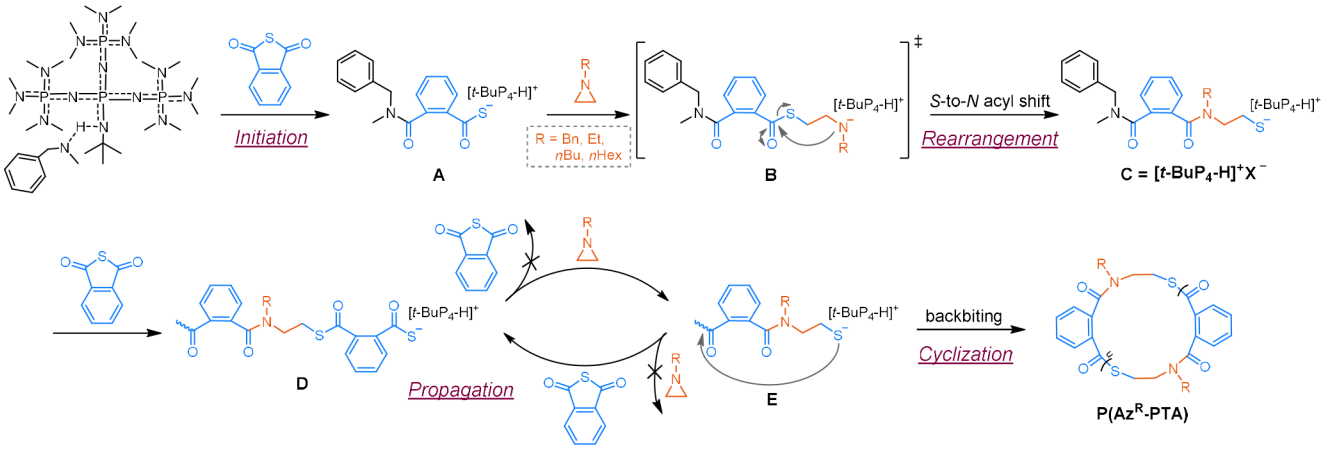

topology and alternating selectivity, although discrepant color changes toward the final yellow color were observed (Figure S1). It is noteworthy that polymerization with the feed order of Az^{Bn}-BnNHMe-*t*-BuP_4-PTA (that is, PTA was added last) showed a slower reaction rate, implying the key role of PTA in the initiating step. More intriguingly, all attempts to prevent the cyclization by adding end-capping reagents (hydrogen chloride, trifluoroacetic acid, trifluoroacetic anhydride, acetyl chloride, iodoacetamide, or benzyl acrylate) in situ in the final stage of polymerization failed. Likewise, Chen and Carpentier et al. reported the formation of cyclic polythioesters in the ROP of thiopropiolactones catalyzed by *t*-BuP_4 or metal catalysts, respectively, and they attributed the cyclization to the backbiting resulting from the much easier transthioesterification than transesterification.[48,60] This mechanism also applies to our ROCOP, as there are abundant thioester bonds in the main chain in addition to the thiolates at the chain end derived from the ring-opening of aziridines and concomitant rearrangement (vide infra).

Notwithstanding, the lingering question remains: when does cyclization occur? To address this, we attempted to synthesize block copolymers via the stepwise addition of different monomer combinations. Specifically, we obtained a diblock copolymer P(Az^{Bn}-PTA)-*b*-P(Az^{nBu}-PTA) through stepwise addition of Az^{nBu}/PTA = 1/1 after Az^{Bn} and PTA had almost consumed, and a triblock copolymer P(Az^{Bn}-PTA)-*b*-P(Az^{nBu}-PTA)-*b*-P(Az^{Bn}-PTA) was produced by further addition of Az^{Bn}/PTA = 1/1. SEC traces for all samples exhibited unimodal distributions and completely shifted in the high-molar-mass direction (Figure 2b). The DOSY NMR spectrum of P(Az^{Bn}-PTA)-*b*-P(Az^{nBu}-PTA)-*b*-P(Az^{Bn}-PTA) exhibited a single diffusion coefficient, verifying the formation of a block polymer instead of polymer mixtures (Figure 2c). Moreover, the ^1H and ^{13}C NMR spectra of the resulting copolymers confirmed the absence of a transthioesterification side reaction (Figures S19 and S20). Overall, well-defined block polymers were obtained due to the high liveness and fidelity of chain ends, even after the complete conversion of monomers and a long reaction period of 64 h. The successful chain extension experiment indicates that the thiolate propagating chain end is stabilized by the protonated base [*t*-BuP_4-H]$^+$ throughout the polymerization (Scheme 2), while cyclization occurs once the electrostatic interaction is destroyed by an external stimulus such as the quenching by "wet" $CDCl_3$ and the precipitation into a poor solvent. The above experiments demonstrate the feasibility and applicability of our ROCOP strategy to construct high-molar-mass macrocycles with excellent selectivity in concentrated solution, which are intriguing polymers with unique and usually better properties than their linear analogs.[61−63]

Finally, LP-TEM was employed to visualize the single molecule, as MALDI-TOF MS is limited in representing the mass information on low-molar-mass polymers due to mass discrimination effects. Thanks to the high molar mass and relatively rigid structure of P(Az^{Bn}-PTA), individual macromolecules were successfully observed, which is a breakthrough for polymers without long side group modification and assembly. As shown in Figure 3a and Movies S1 and S2,

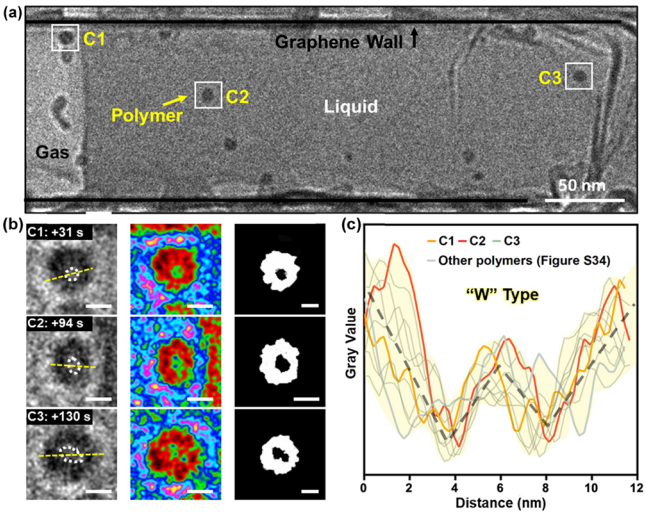

Figure 3. LP-TEM characterization of P(Az^{Bn}-PTA). (a) As-taken TEM image of a 110 nm wide graphene liquid cell containing polymers (M_n = 188.4 kDa, 2 × 10^{-5} mol L^{-1} in DMF), captured at 12.6 s from Movie S1. The scale bar is 50 nm. (b) Representative images of three cyclic polymers (C1−C3) with inner cores highlighted by white dashed lines (left) and a 6-shade false color filter to enhance visual contrast (middle), and their binary images (right). The scale bar is 5 nm. (c) Section analysis of gray value plotted against the position for the yellow dashed lines highlighted in panel (b) and other polymers in Figure S34. The yellow region indicates the uniform trend ("W" type, black dashed line) of gray value curves of different polymers. Imaging conditions: 80 keV, 5 e^-/($Å^2$ s).

https://doi.org/10.1021/acs.macromol.5c00511
Macromolecules 2025, 58, 7686−7696

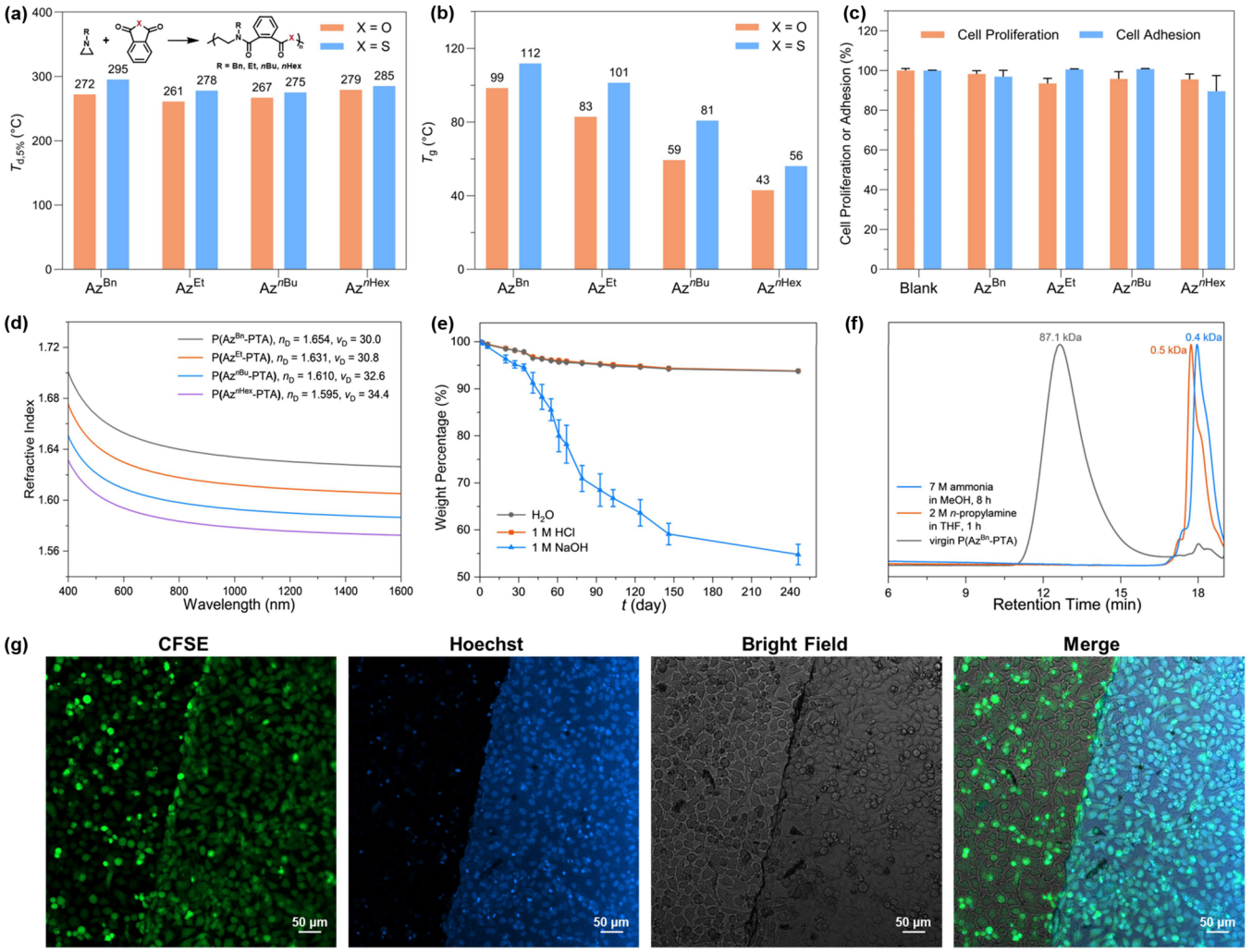

Figure 4. Comparison of (a) $T_{d,5\%}$ and (b) T_g between PEAs and PTEAs. (c) Cell proliferation measured by the MTS assay and cell adhesion on polymer films after 24 h of incubation, relative to the values of blank control, and represented as means ± standard deviation (n = 3). (d) Refractive index plots of PTEAs at various wavelengths. Abbreviation: n = refractive index and υ_D = Abbe number = $(n_D - 1)/(n_F - n_C)$, where n_D, n_F, and n_C are the n values at wavelengths of 589.3, 486.1, and 656.3 nm, respectively. (e) Plots of remaining weight versus exposure time for P(Az^{Bn}-PTA) films exposed to aqueous solutions with different pH values. (f) SEC traces of P(Az^{Bn}-PTA) before and after aminolysis using tetrahydrofuran as the mobile phase, with peak molar masses (M_p) marked in the figure. (g) CLSM images of HeLa cells incubated on the P(Az^{Et}-PTA) film.

polymers were sealed into a graphene liquid cell and dispersed uniformly in the highly diluted good solvent. Zooming in on ten of the nanoparticles, cyclic topology was evidenced for all by analyzing the gray values of the line across the ring (Figures 3b,c and S34), in which the dark domain with lower gray values indicated the existence of polymers with higher electron density (Figure 3b, left), better revealed by a 6-shade false color filter (Figure 3b, middle) and binary methods (Figure 3b, right). "W"-type curves were observed for all polymers, substantiating the hollow ring structure with average outer and inner diameters of 10 and 3 nm, respectively. For comparison, the reaction mixture during the polymerization process was diluted with superdry DMF and imaged under the same conditions. Consistent with our hypothesis, "U" type curves typical of linear polymers were observed (Figure S35). Interestingly, an aggregation process was captured for linear polymers that were spatially adjacent (Figure S36), presumably resulting from the ligation between the active ends of polymers or cross-linking under electron beam irradiation.

Based on the above experimental results and discussion, we deduce that the initiator activated by t-BuP_4 attacks PTA rather than Az^{Bn} first to produce a thiocarboxylate (**A**), which then attacks Az^{Bn} selectively to generate an amine intermediate (**B**). This intermediate then rapidly rearranges via S-to-N acyl shift (N/S exchange) to produce a thiolate chain end (**C**), similar to the natural chemical ligation reaction,[64,65] which subsequently attacks PTA to continue the alternating enchainment, generating a thioester bond at the α terminus and a thiocarboxylate chain end at the ω terminus (**D**). The intramolecular rearrangement of the intermediate was demonstrated by the model reaction with $[Az^{Bn}]_0/[PTA]_0/[t\text{-Bu}P_4]_0/[BnNHMe]_0$ = 10/10/1/10. This reaction yielded a single small-molecule product bearing a sulfhydryl group, identified as the quenched form of species **C** (i.e., **X**−**H**) through NMR and MS characterizations (Figures S13−S18). The efficient rearrangement reaction not only preserves the regular sequence structure but also reverses the relative orientation of the thioester and amide bonds, enabling the final formation of P(Az^R-PTA) in cyclic topology through the intramolecular nucleophilic attack by the thiolate chain end (**E**) at the thioester bond at the α terminus. Indeed, it should be noted that during the polymerization stage, the polymer

https://doi.org/10.1021/acs.macromol.5c00511
Macromolecules 2025, 58, 7686−7696

chain exists in the linear form, with the propagating chain end interacting with the protonated form of bulky superbase [*t*-BuP_4-H]$^+$, which significantly contributes to the excellent selectivity and control over molar mass (Scheme 2).

Thermal and Optical Performance of PTEAs. With four PTEAs in hand, we systematically compared the thermal properties of cyclic PTEAs and previously reported PEAs using thermal gravimetric analysis (TGA) and differential scanning calorimetry (DSC). As depicted in Figure 4a,b, a significant improvement in the thermal performance was achieved by replacing one oxygen atom in the repeat unit with sulfur. Thermal degradation temperatures at 5% weight loss ($T_{d,5\%}$) are elevated to 275−295 °C (Figure S41). Notably, P(Az^{Bn}-PTA) exhibited the highest $T_{d,5\%}$ of 295 °C, surpassing its PEA counterpart by 23 °C. Glass-transition temperatures (T_g), more relevant to material properties, increased by at least 13 °C and could be regulated within the range of 56−112 °C (Figure S42). In general, these PTEAs combine the advantages of thioester and amide bonds, achieving better thermal stability and higher T_gs than their PEA and polythioester analogs (Table S3).[19,50]

Incorporating sulfur atoms or aromatic rings has been proven to elevate the refractive index (n) of polymers by virtue of their high polarizability and molar refraction values.[30,66] Both moieties are present in our PTEAs, resulting in high-refractive-index polymers with n_D values of ≥1.60 (Figure 4d). Among them, P(Az^{Bn}-PTA) with comparable sulfur content but one more benzene ring in the repeat unit shows the highest refractive index of 1.65. To our knowledge, this n_D value is one of the largest refractive indices reported for sulfur-containing polymers obtained through the ROCOP method, surpassing those of polythioethers or polythiocarbonates with much higher sulfur contents[32,53] and polythioesters with the same semiaromatic thioester moiety.[50] Abbe number (υ_D), another important but often overlooked parameter for optical lenses, reflects the wavelength dispersion ability of the materials. However, there is a general trade-off between the n_D and υ_D values of polymers; that is, polymers with high n_D values tend to have low υ_D values. Although a similar trend appears in our system, all of the PTEAs display satisfying υ_D values larger than 30.0, which may arise from the asymmetric backbone structures with randomly distributed *cis*/*trans* repeat units. Moreover, the polymers exhibit excellent optical transparency in the visible and near-infrared regions and strong absorption in the ultraviolet region (Figures S44 and S45), indicating their potential applications as infrared transmitting materials and transparent coatings for blocking ultraviolet radiation.

Degradability and Biocompatibility of PTEAs. With labile bonds in the polymer backbone, thioester-containing polymers often exhibit superior degradability than their ester counterparts and have been proven to degrade under a variety of conditions, such as alkaline hydrolysis, aminolysis, thiolysis, photolysis, and oxidation degradation.[26−29,67] Despite being taken for granted as degradable and biocompatible polymers given the cleavable thioester bond and similar structure to PEAs, few studies have investigated the degradability and biocompatibility of PTEAs, and little is known about the influence of the alternating tertiary amides.[68] In this premise, hydrolysis and aminolysis experiments were conducted for P(Az^{Bn}-PTA). It turned out that polymer films displayed a moderate degradation rate when immersed in a basic aqueous solution due to the hydrophobicity, where the films broke into pieces after 3 weeks and lost ∼45% of their weight after 8 months. In contrast, they remained stable in neutral or acidic systems (Figure 4e). More notably, polymers completely degraded into oligomers featuring molar mass lower than 1 kDa after mixing polymer powders with *n*-propylamine in tetrahydrofuran for 1 h or ammonia in methanol for 8 h due to the densely and evenly distributed thioester bonds in the main chain, although the polymer was initially insoluble in the latter case (Figure 4f).

The evaluation of the cytotoxicity of PTEAs was performed through a cell proliferation assay, followed by the MTS assay (MTS = 3-(4,5-dimethylthiazol-2-yl)-5-(3-carboxymethoxyphenyl)-2-(4-sulfophenyl)-2*H*-tetrazo-lium). It turned out that all four PTEAs showed no cytotoxicity against HeLa cells, as ≥94% cell viability was observed after 48 h in contact with polymers at a concentration of about 1 mg mL^{-1} (Figure 4c). In addition, the confocal laser scanning microscopy (CLSM) images showed that there was scarcely perceptible growth inhibition toward HeLa cells on the polymer films after 24 h of incubation, with the films displaying weak blue emission under a fluorescent microscope (Figures 4c,g and S46−S48). In general, all of these PTEAs exhibited outstanding biocompatibility, showing enormous potential as biomedical materials, particularly considering the excellent degradability of thioesters under manifold conditions.

CONCLUSIONS

This study underscores the feasibility of achieving well-defined PTEAs with diverse functionality through ROCOP of *N*-alkyl aziridines and PTA, facilitated by a phosphazene base and a protic initiator (such as BnSH, BnOH, BnNHMe, and Ph_2CHOH) and via a fancy rearrangement and ring-closure process. In addition to introducing sulfur atoms into the polymer backbone, this approach effectively mitigates several issues pertinent to poor alternating selectivity, low molar mass, and mixed topologies often encountered in analogous copolymerizations involving epoxides or *N*-sulfonyl aziridine.

The spontaneous ROCOP of PTA with Az^{Bn} at 90 °C exhibited a significantly reduced reaction rate along with severe side reactions compared to that of PA. The distinct reactivity between PTA and PA in ROCOP with *N*-alkyl aziridines can be ascribed to the intrinsically lower reactivity of the acyl group in PTA but enhanced nucleophilicity of the thiocarboxylate after PTA ring-opening. By spectroscopy and mass spectrometry analysis, we deciphered the erroneous linkages generated at high temperatures and deduced possible pathways for their formation. The use of organic bases or organic halide salts as catalysts facilitated copolymerization at ambient temperature while simultaneously mitigating undesirable side reactions and enhancing sequence selectivity. Notably, *t*-BuP_4 in conjunction with a protic initiator catalyzed the copolymerization effectively even at a low feed ratio of 0.04 mol %, delivering perfectly alternating cyclic polymers with the highest molar mass of 188.4 kDa over ROCOP thioesters. The macrocycle structure was further confirmed by visualizing the polymers under LP-TEM.

A comprehensive kinetic study by varying the initial concentration of the components elucidated the individual roles of the catalyst and initiator, yielding respective reaction orders of 0.50 for *t*-BuP_4 and 1.32 for BnNHMe. Based on the polymerization and NMR titration results, we propose that *t*-BuP_4 with high basicity and steric hindrance activates the initiator and chain end, while the interaction between the phosphazene cation and chain end anion may account for the

https://doi.org/10.1021/acs.macromol.5c00511
Macromolecules 2025, 58, 7686−7696

high control over copolymerization. Besides, the successful synthesis of block polymers by step-feeding strategy demonstrates that cyclization occurs during the postprocessing, driven by the backbiting of the thiolate chain end resulting from the rapid *S*-to-*N* acyl shift (*N*/*S* exchange).

The incorporation of sulfur confers unique properties on PTEAs, including significant increases of up to 23 °C in $T_{d,5\%}$ and 22 °C in T_g compared with their PEA analogs. Additionally, PTEAs also exhibited higher n_D values and comparable υ_D values relative to their polythioester analogs. Notably, P(Az^{Bn}-PTA) showed the highest $T_{d,5\%}$ of 295 °C and T_g of 112 °C, alongside the exceptional optical performance (n_D = 1.654, υ_D = 30.0), highlighting significant potential as optical materials. Moreover, PTEAs demonstrated favorable degradability via nucleophilic attacks by amines or hydroxyl ions and outstanding biocompatibility toward HeLa cells.

In general, we envisage that not only will the exhaustive discussion on the reaction mechanism presented herein significantly contribute to the ROCOP of *N*/*S*-containing heterocycles but also the facile process and performance-advantaged polymers will promote the synthesis of polymers with similar structures and the exploration of PTEAs as functional materials.

■ ASSOCIATED CONTENT

Supporting Information

The Supporting Information is available free of charge at https://pubs.acs.org/doi/10.1021/acs.macromol.5c00511.

Materials, experimental procedures, additional data, NMR spectra, SEC traces, MALDI-MS spectra, FTIR spectra, LP-TEM images, TGA curves, DSC curves, UV−vis−NIR spectra, CLSM images, and ^{1}H NMR titration for the mechanism (PDF)

Evolution of P(Az^{Bn}-PTA) rings in a typical graphene liquid cell, related to Figure 3 (MP4)

Time-lapsed change of cyclic polymer N9, related to Figure S34 (MP4)

■ AUTHOR INFORMATION

Corresponding Author

Xiaoyan Tang − *Beijing National Laboratory for Molecular Sciences, Key Laboratory of Polymer Chemistry and Physics of Ministry of Education, Center for Soft Matter Science and Engineering, College of Chemistry and Molecular Engineering, Peking University, Beijing 100871, China;* orcid.org/0000-0002-0050-6699; Email: xiaoyan.tang@pku.edu.cn

Authors

Jiaojiao Qin − *Beijing National Laboratory for Molecular Sciences, Key Laboratory of Polymer Chemistry and Physics of Ministry of Education, Center for Soft Matter Science and Engineering, College of Chemistry and Molecular Engineering, Peking University, Beijing 100871, China*

Zhun Xu − *Beijing National Laboratory for Molecular Sciences, Key Laboratory of Polymer Chemistry and Physics of Ministry of Education, National Biomedical Imaging Center, College of Chemistry and Molecular Engineering, Peking University, Beijing 100871, China*

Huan Wang − *Beijing National Laboratory for Molecular Sciences, Key Laboratory of Polymer Chemistry and Physics of Ministry of Education, National Biomedical Imaging Center, College of Chemistry and Molecular Engineering, Peking University, Beijing 100871, China;* orcid.org/0000-0002-2542-936X

Complete contact information is available at: https://pubs.acs.org/10.1021/acs.macromol.5c00511

Notes

The authors declare no competing financial interest.

■ ACKNOWLEDGMENTS

We gratefully acknowledge financial support from the National Natural Science Foundation of China (Nos. 22471006, 52173093, and 22174006) and Beijing Natural Science Foundation (Z240029). We also appreciate Xuan Liang's help in the biocompatibility experiment.

■ REFERENCES

(1) Dequina, H. J.; Jones, C. L.; Schomaker, J. M. Recent Updates and Future Perspectives in Aziridine Synthesis and Reactivity. *Chem.* **2023**, *9*, 1658−1701.

(2) Dank, C.; Ielo, L. Recent Advances in the Accessibility, Synthetic Utility, and Biological Applications of Aziridines. *Org. Biomol. Chem.* **2023**, *21*, 4553−4573.

(3) Sweeney, J. B. Aziridines: Epoxides' Ugly Cousins? *Chem. Soc. Rev.* **2002**, *31*, 247−258.

(4) Gleede, T.; Reisman, L.; Rieger, E.; Mbarushimana, P. C.; Rupar, P. A.; Wurm, F. R. Aziridines and Azetidines: Building Blocks for Polyamines by Anionic and Cationic Ring-Opening Polymerization. *Polym. Chem.* **2019**, *10*, 3257−3283.

(5) Barb, W. G. The Kinetics and Mechanism of the Polymerization of Ethyleneimine. *J. Chem. Soc.* **1955**, 2564−2577.

(6) Gu, G.-G.; Yue, T.-J.; Ren, W. Cationic Ring-Opening Polymerization of *N*-Benzylaziridines to Polyamines via Organic Boron. *Chem. Commun.* **2023**, *59*, 2982−2985.

(7) Stewart, I. C.; Lee, C. C.; Bergman, R. G.; Toste, F. D. Living Ring-Opening Polymerization of *N*-Sulfonylaziridines: Synthesis of High Molecular Weight Linear Polyamines. *J. Am. Chem. Soc.* **2005**, *127*, 17616−17617.

(8) Yang, G.-W.; Xie, R.; Zhang, Y.-Y.; Xu, C.-K.; Wu, G.-P. Evolution of Copolymers of Epoxides and CO_2: Catalysts, Monomers, Architectures, and Applications. *Chem. Rev.* **2024**, *124*, 12305−12380.

(9) Lidston, C. A. L.; Severson, S. M.; Abel, B. A.; Coates, G. W. Multifunctional Catalysts for Ring-Opening Copolymerizations. *ACS Catal.* **2022**, *12*, 11037−11070.

(10) Plajer, A. J.; Williams, C. K. Heterocycle/Heteroallene Ring-Opening Copolymerization: Selective Catalysis Delivering Alternating Copolymers. *Angew. Chem., Int. Ed.* **2022**, *61*, No. e202104495.

(11) Jia, L.; Sun, H.; Shay, J. T.; Allgeier, A. M.; Hanton, S. D. Living Alternating Copolymerization of *N*-Alkylaziridines and Carbon Monoxide as a Route for Synthesis of Poly-*β*-Peptoids. *J. Am. Chem. Soc.* **2002**, *124*, 7282−7283.

(12) Ihata, O.; Kayaki, Y.; Ikariya, T. Synthesis of Thermoresponsive Polyurethane from 2-Methylaziridine and Supercritical Carbon Dioxide. *Angew. Chem., Int. Ed.* **2004**, *43*, 717−719.

(13) Xia, T.; Yue, T.-J.; Gu, G.-G.; Wan, Z.-Q.; Li, Z.-L.; Ren, W.-M. Copolymerization of Aziridines and Cyclic Anhydrides by Metal-Free Catalysis Strategy. *Eur. Polym. J.* **2020**, *136*, No. 109900.

(14) Xu, J.; Hadjichristidis, N. Well-Defined Poly(Ester Amide)-Based Homo- and Block Copolymers by One-Pot Organocatalytic Anionic Ring-Opening Copolymerization of *N*-Sulfonyl Aziridines and Cyclic Anhydrides. *Angew. Chem., Int. Ed.* **2021**, *60*, 6949−6954.

(15) Xu, J.; Wang, X.; Hadjichristidis, N. Diblock Dialternating Terpolymers by One-Step/One-Pot Highly Selective Organocatalytic Multimonomer Polymerization. *Nat. Commun.* **2021**, *12*, 7124.

(16) Xu, J.; Zhang, P.; Yuan, Y.; Hadjichristidis, N. Elucidation of the Alternating Copolymerization Mechanism of Epoxides or Aziridines with Cyclic Anhydrides in the Presence of Halide Salts. *Angew. Chem., Int. Ed.* **2023**, *62*, No. e202218891.

(17) Gao, T.; Li, F.; Suzuki, R.; Li, H.; Yamamoto, T.; Xia, X.; Isono, T.; Satoh, T. One-Step Synthesis of Poly(Amide Ester)-Based Block Copolymers with Defined Phase Separation Behavior. *Macromolecules* **2023**, *56*, 8333−8343.
(18) Gao, T.; Xia, X.; Watanabe, T.; Ke, C.-Y.; Suzuki, R.; Yamamoto, T.; Li, F.; Isono, T.; Satoh, T. Toward Fully Controllable Monomers Sequence: Binary Organocatalyzed Polymerization from Epoxide/Aziridine/Cyclic Anhydride Monomer Mixture. *J. Am. Chem. Soc.* **2024**, *146*, 25067−25077.
(19) Qin, J.; Tang, X. Toward Catalyst-Free Synthesis of Tough Cyclic Poly(Ester Amide)s: Alternating Copolymerization of Aziridines and Phthalic Anhydride. *Macromolecules* **2023**, *56*, 8666−8675.
(20) Han, S.; Wu, J. Recent Advances of Poly(Ester Amide)s-Based Biomaterials. *Biomacromolecules* **2022**, *23*, 1892−1919.
(21) Ranganathan, P.; Chen, C.-W.; Rwei, S.-P.; Lee, Y.-H.; Ramaraj, S. K. Methods of Synthesis, Characterization and Biomedical Applications of Biodegradable Poly(Ester Amide)s- A Review. *Polym. Degrad. Stab.* **2020**, *181*, No. 109323.
(22) Song, P.-D.; Xia, L.; Nie, X.; Chen, G.; Wang, F.; Zhang, Z.; Hong, C.-Y.; You, Y.-Z. Synthesis of Poly(Thioester Sulfonamide)s via the Ring-Opening Copolymerization of Cyclic Thioanhydride with *N*-Sulfonyl Aziridine Using Mild Phosphazene Base. *Macromol. Rapid Commun.* **2022**, *43*, No. 2200140.
(23) Fornacon-Wood, C.; Manjunatha, B. R.; Stühler, M. R.; Gallizioli, C.; Müller, C.; Pröhm, P.; Plajer, A. J. Precise Cooperative Sulfur Placement Leads to Semi-Crystallinity and Selective Depolymerisability in CS_2/Oxetane Copolymers. *Nat. Commun.* **2023**, *14*, 4525.
(24) Yuan, P.; Sun, Y.; Xu, X.; Luo, Y.; Hong, M. Towards High-Performance Sustainable Polymers via Isomerization-Driven Irreversible Ring-Opening Polymerization of Five-Membered Thionolactones. *Nat. Chem.* **2022**, *14*, 294−303.
(25) Zhao, J.-Z.; Yue, T.-J.; Ren, B.-H.; Liu, Y.; Ren, W.-M.; Lu, X.-B. Recyclable Sulfur-Rich Polymers with Enhanced Thermal, Mechanical, and Optical Performance. *Macromolecules* **2022**, *55*, 8651−8658.
(26) Abu Bakar, R.; Hepburn, K. S.; Keddie, J. L.; Roth, P. J. Degradable, Ultraviolet-Crosslinked Pressure-Sensitive Adhesives Made from Thioester-Functional Acrylate Copolymers. *Angew. Chem., Int. Ed.* **2023**, *62*, No. e202307009.
(27) Stephan, J.; Stühler, M. R.; Rupf, S. M.; Neale, S.; Plajer, A. J. Mechanistic Mapping of (CS_2/CO_2)/Epoxide Copolymerization Catalysis Leads to Terpolymers with Improved Degradability. *Cell Reports Phys. Sci.* **2023**, *4*, No. 101510.
(28) Fornacon-Wood, C.; Stühler, M. R.; Gallizioli, C.; Manjunatha, B. R.; Wachtendorf, V.; Schartel, B.; Plajer, A. J. Precise Construction of Weather-Sensitive Poly(Ester-*alt*-Thioesters) from Phthalic Thioanhydride and Oxetane. *Chem. Commun.* **2023**, *59*, 11353−11356.
(29) Kiel, G. R.; Lundberg, D. J.; Prince, E.; Husted, K. E. L.; Johnson, A. M.; Lensch, V.; Li, S.; Shieh, P.; Johnson, J. A. Cleavable Comonomers for Chemically Recyclable Polystyrene: A General Approach to Vinyl Polymer Circularity. *J. Am. Chem. Soc.* **2022**, *144*, 12979−12988.
(30) Mazumder, K.; Voit, B.; Banerjee, S. Recent Progress in Sulfur-Containing High Refractive Index Polymers for Optical Applications. *ACS Omega* **2024**, *9*, 6253−6279.
(31) Zhang, J.; Bai, T.; Liu, W.; Li, M.; Zang, Q.; Ye, C.; Sun, J. Z.; Shi, Y.; Ling, J.; Qin, A.; Tang, B. Z. All-Organic Polymeric Materials with High Refractive Index and Excellent Transparency. *Nat. Commun.* **2023**, *14*, 3524.
(32) Yue, T.-J.; Ren, B.-H.; Zhang, W.-J.; Lu, X.-B.; Ren, W.-M.; Darensbourg, D. J. Randomly Distributed Sulfur Atoms in the Main Chains of CO_2-Based Polycarbonates: Enhanced Optical Properties. *Angew. Chem., Int. Ed.* **2021**, *60*, 4315−4321.
(33) Kim, D. H.; Jang, W.; Choi, K.; Choi, J. S.; Pyun, J.; Lim, J.; Char, K.; Im, S. G. One-Step Vapor-Phase Synthesis of Transparent High Refractive Index Sulfur-Containing Polymers. *Sci. Adv.* **2020**, *6*, No. eabb5320.
(34) Kleine, T. S.; Lee, T.; Carothers, K. J.; Hamilton, M. O.; Anderson, L. E.; Ruiz Diaz, L.; Lyons, N. P.; Coasey, K. R.; Parker, W. O.; Borghi, L.; Mackay, M. E.; Char, K.; Glass, R. S.; Lichtenberger, D. L.; Norwood, R. A.; Pyun, J. Infrared Fingerprint Engineering: A Molecular-Design Approach to Long-Wave Infrared Transparency with Polymeric Materials. *Angew. Chem., Int. Ed.* **2019**, *58*, 17656−17660.
(35) Griebel, J. J.; Namnabat, S.; Kim, E. T.; Himmelhuber, R.; Moronta, D. H.; Chung, W. J.; Simmonds, A. G.; Kim, K.; van der Laan, J.; Nguyen, N. A.; Dereniak, E. L.; Mackay, M. E.; Char, K.; Glass, R. S.; Norwood, R. A.; Pyun, J. New Infrared Transmitting Material via Inverse Vulcanization of Elemental Sulfur to Prepare High Refractive Index Polymers. *Adv. Mater.* **2014**, *26*, 3014−3018.
(36) Zheng, N.; Xu, Y.; Zhao, Q.; Xie, T. Dynamic Covalent Polymer Networks: A Molecular Platform for Designing Functions beyond Chemical Recycling and Self-Healing. *Chem. Rev.* **2021**, *121*, 1716−1745.
(37) Cao, W.; Dai, F.; Hu, R.; Tang, B. Z. Economic Sulfur Conversion to Functional Polythioamides through Catalyst-Free Multicomponent Polymerizations of Sulfur, Acids, and Amines. *J. Am. Chem. Soc.* **2020**, *142*, 978−986.
(38) Tian, T.; Hu, R.; Tang, B. Z. Room Temperature One-Step Conversion from Elemental Sulfur to Functional Polythioureas through Catalyst-Free Multicomponent Polymerizations. *J. Am. Chem. Soc.* **2018**, *140*, 6156−6163.
(39) Sun, Q.; Aguila, B.; Perman, J.; Earl, L. D.; Abney, C. W.; Cheng, Y.; Wei, H.; Nguyen, N.; Wojtas, L.; Ma, S. Postsynthetically Modified Covalent Organic Frameworks for Efficient and Effective Mercury Removal. *J. Am. Chem. Soc.* **2017**, *139*, 2786−2793.
(40) Feng, G.; Feng, X.; Liu, X.; Guo, W.; Zhang, C.; Zhang, X. Metal-Free Alternating Copolymerization of CS_2 and Oxetane. *Macromolecules* **2023**, *56*, 6798−6805.
(41) Sun, Y.; Zhang, C.; Zhang, X. O/S Exchange Reaction in Synthesizing Sulfur-Containing Polymers. *Chem.—Eur. J.* **2024**, *30*, No. e202401684.
(42) Yue, T.-J.; Ren, W.-M.; Lu, X.-B. Copolymerization Involving Sulfur-Containing Monomers. *Chem. Rev.* **2023**, *123*, 14038−14083.
(43) Purohit, V. B.; Pięta, M.; Pietrasik, J.; Plummer, C. M. Recent Advances in the Ring-Opening Polymerization of Sulfur-Containing Monomers. *Polym. Chem.* **2022**, *13*, 4858−4878.
(44) Li, H.; Guillaume, S. M.; Carpentier, J. Polythioesters Prepared by Ring-Opening Polymerization of Cyclic Thioesters and Related Monomers. *Chem.—Asian J.* **2022**, *17*, No. e202200641.
(45) Yue, T.-J.; Wang, L.-Y.; Ren, W.-M. The Synthesis of Degradable Sulfur-Containing Polymers: Precise Control of Structure and Stereochemistry. *Polym. Chem.* **2021**, *12*, 6650−6666.
(46) Chen, X.-L.; Wang, B.; Song, D.-P.; Pan, L.; Li, Y.-S. One-Step Synthesis of Sequence-Controlled Polyester-*Block*-Poly(Ester-*alt*-Thioester) by Chemoselective Multicomponent Polymerization. *Macromolecules* **2022**, *55*, 1153−1164.
(47) Narmon, A. S.; van Slagmaat, C. A. M. R.; De Wildeman, S. M. A.; Dusselier, M. Sustainable Polythioesters via Thio(no)lactones: Monomer Synthesis, Ring-Opening Polymerization, End-of-Life Considerations, and Industrial Perspectives. *ChemSusChem* **2023**, *16*, No. e202202276.
(48) Li, H.; Ollivier, J.; Guillaume, S. M.; Carpentier, J. Tacticity Control of Cyclic Poly(3-Thiobutyrate) Prepared by Ring-Opening Polymerization of Racemic β-Thiobutyrolactone. *Angew. Chem., Int. Ed.* **2022**, *61*, No. e202202386.
(49) Bannin, T. J.; Kiesewetter, M. K. Poly(Thioester) by Organocatalytic Ring-Opening Polymerization. *Macromolecules* **2015**, *48*, 5481−5486.
(50) Wang, L.-Y.; Gu, G.-G.; Yue, T.-J.; Ren, W.-M.; Lu, X.-B. Semiaromatic Poly(Thioester) from the Copolymerization of Phthalic Thioanhydride and Epoxide: Synthesis, Structure, and Properties. *Macromolecules* **2019**, *52*, 2439−2445.
(51) Wang, L.-Y.; Gu, G.-G.; Ren, B.-H.; Yue, T.-J.; Lu, X.-B.; Ren, W.-M. Intramolecularly Cooperative Catalysis for Copolymerization

of Cyclic Thioanhydrides and Epoxides: A Dual Activation Strategy to Well-Defined Polythioesters. *ACS Catal.* **2020**, *10*, 6635−6644.
(52) Rupf, S.; Pröhm, P.; Plajer, A. J. Lithium Achieves Sequence Selective Ring-Opening Terpolymerisation (ROTERP) of Ternary Monomer Mixtures. *Chem. Sci.* **2022**, *13*, 6355−6365.
(53) Zhang, C.-J.; Zhu, T.-C.; Cao, X.-H.; Hong, X.; Zhang, X.-H. Poly(Thioether)s from Closed-System One-Pot Reaction of Carbonyl Sulfide and Epoxides by Organic Bases. *J. Am. Chem. Soc.* **2019**, *141*, 5490−5496.
(54) Diebler, J.; Komber, H.; Häußler, L.; Lederer, A.; Werner, T. Alkoxide-Initiated Regioselective Coupling of Carbon Disulfide and Terminal Epoxides for the Synthesis of Strongly Alternating Copolymers. *Macromolecules* **2016**, *49*, 4723−4731.
(55) Tran, D. K.; Braaksma, A. N.; Andras, A. M.; Boopathi, S. K.; Darensbourg, D. J.; Wooley, K. L. Structural Metamorphoses of *D*-Xylose Oxetane- and Carbonyl Sulfide-Based Polymers In Situ during Ring-Opening Copolymerizations. *J. Am. Chem. Soc.* **2023**, *145*, 18560−18567.
(56) Guo, Y.-T.; Xiong, W.; Shi, C.; Du, F.-S.; Li, Z.-C. Facile Synthesis of Eight-Membered Cyclic (Ester-Amide)s and Their Organocatalytic Ring-Opening Polymerizations. *Polym. Chem.* **2022**, *13*, 4490−4501.
(57) Hong, M.; Chen, E. Y.-X. Towards Truly Sustainable Polymers: A Metal-Free Recyclable Polyester from Biorenewable Non-Strained γ-Butyrolactone. *Angew. Chem., Int. Ed.* **2016**, *55*, 4188−4193.
(58) Yue, T.-J.; Zhang, M.-C.; Gu, G.-G.; Wang, L.-Y.; Ren, W.-M.; Lu, X.-B. Precise Synthesis of Poly(Thioester)s with Diverse Structures by Copolymerization of Cyclic Thioanhydrides and Episulfides Mediated by Organic Ammonium Salts. *Angew. Chem., Int. Ed.* **2019**, *58*, 618−623.
(59) Yang, R.; Wang, Y.; Luo, W.; Jin, Y.; Zhang, Z.; Wu, C.; Hadjichristidis, N. Carboxylic Acid Initiated Organocatalytic Ring-Opening Polymerization of *N*-Sulfonyl Aziridines: An Easy Access to Well-Controlled Polyaziridine-Based Architectural and Functionalized Polymers. *Macromolecules* **2019**, *52*, 8793−8802.
(60) Zhou, L.; Reilly, L. T.; Shi, C.; Quinn, E. C.; Chen, E. Y.-X. Proton-Triggered Topological Transformation in Superbase-Mediated Selective Polymerization Enables Access to Ultrahigh-Molar-Mass Cyclic Polymers. *Nat. Chem.* **2024**, *16*, 1357−1365.
(61) Ochs, J.; Pagnacco, C. A.; Barroso-Bujans, F. Macrocyclic Polymers: Synthesis, Purification, Properties and Applications. *Prog. Polym. Sci.* **2022**, *134*, No. 101606.
(62) Haque, F. M.; Grayson, S. M. The Synthesis, Properties and Potential Applications of Cyclic Polymers. *Nat. Chem.* **2020**, *12*, 433−444.
(63) Cortez, M. A.; Godbey, W. T.; Fang, Y.; Payne, M. E.; Cafferty, B. J.; Kosakowska, K. A.; Grayson, S. M. The Synthesis of Cyclic Poly(Ethylene Imine) and Exact Linear Analogues: An Evaluation of Gene Delivery Comparing Polymer Architectures. *J. Am. Chem. Soc.* **2015**, *137*, 6541−6549.
(64) Dawson, P. E.; Muir, T. W.; Clark-Lewis, I.; Kent, S. B. H. Synthesis of Proteins by Native Chemical Ligation. *Science* **1994**, *266*, 776−779.
(65) Agouridas, V.; El Mahdi, O.; Diemer, V.; Cargoët, M.; Monbaliu, J.-C. M.; Melnyk, O. Native Chemical Ligation and Extended Methods: Mechanisms, Catalysis, Scope, and Limitations. *Chem. Rev.* **2019**, *119*, 7328−7443.
(66) Higashihara, T.; Ueda, M. Recent Progress in High Refractive Index Polymers. *Macromolecules* **2015**, *48*, 1915−1929.
(67) Bingham, N. M.; un Nisa, Q.; Chua, S. H. L.; Fontugne, L.; Spick, M. P.; Roth, P. J. Thioester-Functional Polyacrylamides: Rapid Selective Backbone Degradation Triggers Solubility Switch Based on Aqueous Lower Critical Solution Temperature/Upper Critical Solution Temperature. *ACS Appl. Polym. Mater.* **2020**, *2*, 3440−3449.
(68) Becker, G.; Wurm, F. R. Functional Biodegradable Polymers via Ring-Opening Polymerization of Monomers without Protective Groups. *Chem. Soc. Rev.* **2018**, *47*, 7739−7782.

https://doi.org/10.1021/acs.macromol.5c00511
Macromolecules 2025, 58, 7686−7696